Applied Thermal Engineering 258 (2025) 124774

Contents lists available at ScienceDirect

Applied Thermal Engineering

journal homepage: www.elsevier.com/locate/apthermeng

Research Paper

Model-based assessment of a feedforward-feedback control strategy for ORC-based unit in waste heat recovery application

Fabio Fatigati *, Davide Di Battista, Roberto Carapellucci

University of L'Aquila, Department of Industrial Engineering and Economics, Piazzale Ernesto Pontieri, L'Aquila 67100, Italy

ARTICLE INFO

Keywords:
ORC-based power unit control system
Feedforward and feedback regulating system
Waste heat recovery
Scroll expander
Internal combustion engine

ABSTRACT

Research in the automotive sector is driven by the need to reduce the greenhouse gases emissions, while maintaining the expected vehicle performances. The electrification and hybridization ensure to achieve this goal, anyway, some issues still limit their full development in the international panorama. For this reason, the technological improvement of Internal Combustion Engines (ICEs) plays a crucial role in this transition period, also considering the opportunities related to sustainable fuels. Among the technological solutions allowing to improve ICEs performances, the energy recovery from the exhaust gases through Organic Rankine Cycle (ORC)-based power units are one of the most attractive alternatives, due to the high enthalpic content of the hot source. Despite these benefits, the ICE exhaust gases usually have considerable fluctuation of thermodynamic conditions. For this reason, it is necessary the adoption of a reliable and robust control system to keep the main operating ORC quantities (superheating degree, expander intake pressure and temperature) within a suitable and safe range. ORC control strategies for transportation applications are often based on detailed models that predict the unit behaviour, making use of Proportional-Integrative-Derivative (PID) regulators, whose coefficients are generally tuned through theoretical approaches and dedicated software. In the present work, an innovative control system has been developed, based on the integration of a feedforward (FF) and proportional feedback (FDB) regulating strategies. Despite the simplicity of the proposed approach, it ensures the proper plant operation even under severe fluctuations of the hot source. Particularly, the gain of FDB is based on a constitutive relationship between the expander intake pressure and working fluid mass flow rate. Such gain, indeed, is universally valid, not requiring to be tuned as generally done. The benefits of the proposed strategy are assessed thanks to a comprehensive model of the whole ORC unit, validated through experimental data carried out on a fully instrumented test bench in dynamic working conditions. Results demonstrate the robustness of the feedforward-proportional regulating approach: a superheating degree of 15–20 °C is ensured, keeping the plant power and efficiency close to the design value (1 to2 kW and 4 to6% respectively) even in off-design conditions. Moreover, the safe operating of the expander is guaranteed limiting the maximum temperature excursion under the safety limit of 160 °C.

1. Introduction

Transportations represents the 22 % of the whole CO_2 emissions in the energy sector with the on-the road transport covering a share of 73.5 % [1]. Indeed, the needs of CO_2 reduction is one of the main objectives of the International Community, as European Union which in European Green Deal defines the strategy to face the climate change and achieving the carbon neutrality by 2050 [2]. This pushes the research in this sector to find new technologies able to reduce the CO_2 emissions and guaranteeing at the same time the expected performance. In this perspective, the electric vehicles are pushed to a widespread diffusion with sales that in 2022 increase in a share of 75 % with respect to 2021 [3]. Nevertheless, real environmental benefits are achieved only if the electricity in the grid is carbon-free, but the whole renewable share growth is still not sufficient to decarbonize the sector entirely [4]. Indeed, it is forecasted that by 2050 renewables cover only a share of 44 % of the grid electricity [4]. Hence, the transition towards a carbon natural transportation sector should be pursued considering also carbon reduction technique for the Internal Combustion Engines (ICEs), which will remain the most used powertrain system, in particular for medium-heavy duty transportation vehicles, [5]. Again, suitable solutions are the adoption of synthetic or

* Corresponding author.
E-mail address: fabio.fatigati@univaq.it (F. Fatigati).

https://doi.org/10.1016/j.applthermaleng.2024.124774
Received 4 August 2024; Received in revised form 8 October 2024; Accepted 30 October 2024
Available online 1 November 2024

Nomenclature

Symbols

A	Surface [m^2]
c_p	specific heat at constant pressure [kJ/kgK]
e	FDB error between SP and actual expander intake pressure [bar], [MPa]
h	specific enthalpy [kJ/kg]
k	slope of the linear relation between expander intake pressure and mass flow rate [bar/kg/s]
k''	pressure error/pump speed constant [rpm/bar], [rpm/MPa]
$k_{m\omega}$	mass flow rate/pump speed constant [RPM/kg/s]
LMDT	Logarithmic mean temperature difference [K]-[°C]
$\dot{m}$	mass flow rate [kg/s], [g/s]
P	Power [kW], [W]
Q	y-axis intercept of the linear relation between expander intake pressure and mass flow rate [bar]
Q	thermal power [kW]
RMSE	Root Mean Square Error
RMSEr	Relative Root Mean Square Error
Sat	saturation
SD	Standard deviation
SP	set point
T	temperature [°C], [K]
T	time [s]
U	heat transfer coefficient [W/m^2K]
V	volume [m^3]

Subscripts

Disp	displaced volume
Exp	expander
exh,gas	exhaust gases
FDB	Feedback
FF	Feedforward
HRVG	Heat Recovery Vapor Generator
In	inlet
ORC	Organic Rankine Cycle
Actual	actual value of expander intake pressure
Out	outlet
Pmp	pump
Rec	recovered
Vol	volumetric
W	water
Wall	metallic masses wall
WF	working fluid

Greek letters

$\Delta\omega_{pmp}$	pump speed variation [rpm]
ΔT_{SH}	superheating degree [°C], [K]
η	efficiency
ρ	density [kg/m^3]
ω	revolution speed [RPM]

bio-based fuels [6,7], or lower carbon intensity hydrogen [8–10], which consent to keep the existing components, without great changes in the powertrain.

Therefore, the technological improvement of Internal Combustion Engines still plays a strategic role in this transition period [11]. Waste Heat Recovery (WHR) applications represent an interesting solution to improve the ICEs gross efficiency as the quite total amount of energy loss is reversed to the exhaust gases and cooling medium [12]. Among WHR solutions [13–15], those referred to Organic Rankine Cycle (ORC)-based units are widely studied thanks to their reliability, adaptability and stable performance [16]. Despite this benefits, the frequent and wide fluctuation of the waste heat (i.e. exhaust gases) involves significant difficulties and challenges on the dynamic and control of the ORC-based power unit [17]. A proper control system is essential to guarantee satisfactory recovery performance and operating constraints to avoid plant damage. One operating constraint refers to working fluid (WF) temperature which must be kept below the degradation limit. Another is related to the WF maximum pressure that must be kept under the maximum value allowed by the mechanical components [17]. Nonetheless, only few works about control and regulating system of ORC-based power units for waste heat recovery applications are available [18]. Proportional Integrative Derivative (PID) control strategies are widely adopted [19]. In [20], different regulating strategies based on Proportional-Integrative (PI) controller are developed considering as control parameters the speed of the pump and expander. The best results are achieved considering as regulating parameter the evaporating temperature optimized through a steady-state model. In [21], different control strategies are compared considering different manipulated variables (pump speed, turbine speed, pump and turbine speed contemporaneously). The PI controller is developed based on the step response of the ORC-based unit. Turbine based regulating strategy presents the best results in terms of thermodynamic behaviour whereas the pump-based one allows to keep the output power close to the rated point. In [22], PID regulation strategies was developed for long haul truck. The PID coefficients are set through Matlab® PID tuner application, and it manipulated variable pump speed, bypass valve at evaporator exhaust gas entrance, used alternatively to a throttling valve on the turbine inlet. Results show that the handling of the pump speed and a throttling valve at expander inlet allows to achieve better performance than a control based on pump speed and the exhaust gases valve actuation. In [23], PI regulator was tuned through the Ziegler-Nichols method considering as manipulated variable and control variables respectively the pump and expander speed. In that work PI was integrated with feedforward and lead-lag compensation to guarantee a faster reaction of the system. In [24] the operating parameters like evaporating and condensing pressure are internally optimized and a PID was adopted as regulator. The control system allows to keep the superheating degree at expander inlet in a range comprised between 5 and 15 °C thus avoiding undesirable start and stop procedure.

Despite the wide adoption of PID regulators, it was seen that high deviation in terms of superheating degree are experienced in case of a rapid variation of heat source [25]. This evidence pushes the interest and research on more advanced controls like the Optimal Control (OC) and Model Predictive Controls (MPC) strategies [19].

Optimal Controls are based on ORC-based power unit model used to represent the path of the control variable with objective functions like thermal efficiency, power output, closed loop tracking error, etc. In [26], a controller was designed to maximize the recovered energy of an ORC-based unit fed by the waste heat of a diesel-electric train. The net power output is maximized acting on the by-pass valve on the exhaust gases and on the mass flow rate of condensing air. The OC problem is related to a simplified model of the plant solved by dynamic programming featured by adaptive grid with evaporator and condenser modelled as single-state system. In a subsequent work [27], the issue of real time operating was solved with the dynamic programming adopted to supervise the system. A single objective optimization was adopted in [28] to keep the superheating degree of working fluid at turbine inlet close to the set point for a wide disturbance related to the mass flow rate and temperature fluctuation of the hot source. The proposed algorithm presents a smaller overshoot and settling time compared to a PID tuned in

Matlab environment.

Model Predictive Control (MPC) is a control approach to regulate multi-variable system satisfying a set of constraints and it attracts a significant interest in the last year [29,30]. MPC is based on linearization similarly to Linear Quadratic Regulators (LQR), but it provides a control optimization only for a limited prevision horizon, repeating at every step the optimization procedure [17]. Despite MPC offers better performance than PID regulation [31], the comparisons were carried out for small step change and condition generally far from the real ones [32]. Moreover, the higher computational cost and complexity could not justify its adoption [26].

Compared to advanced control systems, feedforward (FF)/feedback (FDB) controls can introduce significant benefits. Indeed, they do not require an online optimization and the uncertainty introduced by modelling and measurement errors, while system aging can be addressed by feedback part [17] Despite the simplicity of this control approach only few analyses are focused on this topic for Waste Heat Recovery application [18]. An inversed feedforward control system based on an inverted Moving Boundary (MB) model of the evaporator was adopted in [33] to control the superheating degree of working fluid at expander inlet. The pump speed was determined to achieve a desired value of superheating degree and experimental analysis assess the better performance with respect to a PID regulating system. A feedforward regulating strategy based on a four-order evaporator MB model coupled with a volumetric expander was adopted in [34]. Results shows higher fluctuation in terms of superheating (−15/60 K), nevertheless, the integration of FF section with a LQR allows to achieve at least an improvement of 25 % in terms of thermal efficiency with respect to other solutions (integration with PI feedback or static feedforward). In [35], a feedforward, a PID and a combined feedforward and PID regulating strategies were compared to regulate a biomass-fired ORC-based unit. The best performances are achieved using the combined regulating system. In [17], a novel approach to integrate a dynamic-non linear feedforward control model with a classical PI control system was developed for an ORC-based unit feed by ICE exhaust gases. High order MB model was considered with innovative numerical approximation. An important aspect treated by this work is the evaluation of the control effort about the possibility to introduce pump failure and lifetime reduction.

It was observed in literature that PID feedback controller with tuned coefficients is not able to keep the superheating degree at expander inlet close without an error lower than ± 30 K [22]. In this work, a novel regulating approach for an ORC-based recovery unit is presented, in order to improve the performance of a feedback regulator without recurring to the integration with high order MB model. This consent to apply the control strategy also to high speed variation of the boundary conditions (i.e. waste heat recovery thermodynamic fluctuations).

It is based on the integration of a static feedforward (FF) /feedback (FDB) sections developed to control the superheating degree of the working fluid at expander intake acting on the pump speed. The main novelty introduced by the present research is that the intrinsic relationship between expander intake pressure and working fluid mass flow rate is adopted to define the FDB proportional coefficient (gain). This allows to avoid the tuning process of the parameter through PID tune program or theoretical approach. Up to date, the regulating coefficient have been tuned recurring to specific algorithms or software routines such as Matlab Simulink. In the present research, the control of the entire system is based on the intrinsic regulation of expander intake pressure and working fluid mass flow rate given by the plant permeability. Indeed, according to the authors' findings in their previous work [36], when a volumetric expander is used, it behaves like a revolving valve. Hence, the lower its permeability the greater is the pressure enhancement for a given mass flow rate increase, and vice versa. Permeability is defined as the ratio between the working fluid mass flow rate and the expander intake pressure. If the expander speed is not externally varied, permeability undergoes low variation and can be retained constant, hence, the relation between the expander intake pressure and working fluid mass flow rate is linear. This was used in this work as the base of the proportional feedback regulation whose novelty is that the coefficient is univocally defined based on the expander operating feature.

Moreover, a further novelty is related to the control approach adopted. In fact, the simplicity of the regulating strategy is privileged, accepting a certain regulating error. This is since the frequent variation of the hot source and the thermal inertia of the ORC-based unit involve that the need to ensure the operating quantities, such as maximum temperature and superheating degree at expander intake, are within prescribed range is most important that a given value is reached. In particular, the maximum temperature of working fluid must be lower than minimum value between the decomposition temperature of working fluid and the maximum allowable value for the components material. Thanks to the self-regulating capacity of the volumetric expander, the plant can absorb slight variation of the main operating quantities (such as superheating degree at its inlet). In other words, due to the operating flexibility of the plant, achieved thanks to the adoption of a volumetric expander, satisfying performances are reached even if a certain error is encountered on the controlled quantities (i.e. superheating degree) within a prescribed range. This knowledge allows to simplify the control system and consequently the computational resource and time needed.

In order to demonstrate the effectiveness and benefits introduced by the proposed regulating strategy, a comprehensive model of the unit was adopted. The model was experimentally validated against experimental data characterizing the plant dynamic behaviour to the step-variation of ICE operating conditions. The experimental data are collected on a fully instrumented ORC-based unit fed by the exhaust gases of an Internal Combustion Engine. The analysis of the experimental data allows to put in light relationship between the main operating quantities ensuring a simplification of the intrinsic non-linear behaviour of the ORC-based unit. Once validated the model was used to compare the benefits introduced by the regulating strategy over a severe and sudden fluctuation of the hot source represented by the exhaust gas of a 3 Liters (L) supercharged Diesel engine.

2. Materials and methods

2.1. Experimental test-bench

In order to support the activity, a wide experimental characterization of a fully instrumented Organic Rankine Cycle (ORC) power unit was developed under dynamic working conditions. The ORC-based unit (Fig. 1) was developed to be fed by the exhaust gases of a 3 L supercharged Diesel Engine (IVECO F1C) installed on a dynamic test bench (a). This allows to reproduce the real ICE operation and observe the ORC-based unit dynamic response to the pulsation of the heat source represented by the exhaust gases of the ICE.

The exhaust gases flow in the hot side of a Heat Recovery Vapor Generator (HRVG, (b) thus providing thermal power to the working fluid (WF) flowing in the HRVG cold side. As working fluid, R245fa was selected mixed with ISOVG68 POE oil in amount of 5 % of the total mass charge of R245fa (5 kg). The WF exits the HRVG as a 10–20 K superheated value and enters in a 1 kW hermetic Scroll expander (c) whose generator is connected to a resistive electric load (d). Indeed, scroll generator produces a 3-phase voltage, which is converted in a DC voltage by an AC/DC converter and dissipated thanks to a variable electric resistance. Once expanded, the working fluid enters into a plate heat exchanger (e) where the WF, cooled by tap water, is condensed and subcooled. Prior to be pumped by a gear rotor pump, the WF is gathered inside a 3 L tank (f), placed upstream the pump (g) to avoid cavitation and dump fluctuation at higher flow rates.

Concerning the experimental measurement instruments, upstream and downstream each components pressure transducers and

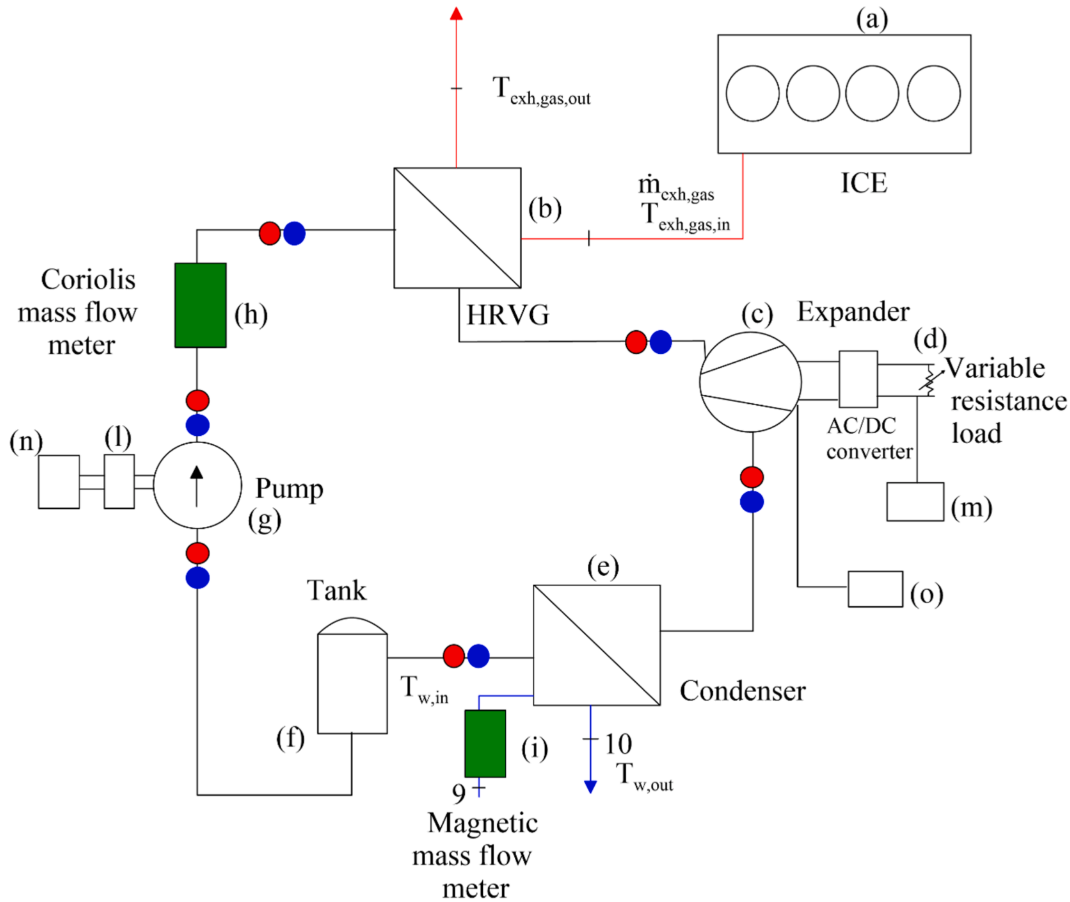

Fig. 1. Scheme of the fully instrumented ORC-based power unit fed by the exhaust gases of an Internal Combustion Engine. Blue and red circles are pressure and temperature sensors.

thermocouples are introduced to reconstruct the thermodynamic cycle. The working fluid mass flow rate is measured through a Coriolis mass flow meter (h), whereas the tap water flow rate in the condenser is measured via a magnetic one (i). The exhaust gases and ICE parameter are taken from the Electric Control Unit (ECU) of the system. Pump power is measured through a dedicated torque-meter (l) whereas the expander power measuring the DC electric variables on the electric load (m). Thanks to a dedicated inverter placed on the pump electric motor (n), the pump speed can be set to define the desired working fluid mass flow rate. The expander speed is instead evaluated introducing a magnetic probe inside the casing reporting the measurement on a dedicated oscilloscope (o). In Table 1, the measurement uncertainties are reported.

Table 1
Measurement Uncertainties of the adopted instruments.

Instrument	Quantity	Uncertainty
Coriolis Mass-flow rate	Working fluid mass flow rate	±0.15 % of the measured value
Magnetic mass flow rate	Water mass flow rate	±0.5 % of the measured value
Pump torque meter	Torque/Revolution speed	0.02 Nm/ 1 RPM
T-Thermocouple	Working fluid temperature	0.3 °C
K-Thermocouple	Exhaust gases temperature	2.2 °C
Pressure sensor	Working fluid pressure	0.3 bar
Current sensor	DC current (electric load)	1 % of FS-(0.1 A)
Voltage sensor	DC voltage (electric load)	0.6 % of FS, 4.2 Volt

2.2. 2.2.Mathematical model

The benefits introduced by the proposed regulating strategy is assessed thanks to a comprehensive theoretical model of the whole unit [36]. The model is based on the integration of zero (0D) and mono (1-D) dimensional thermo-fluid-dynamic analysis and allows to reproduce the physical behaviour of the whole unit.

1D analysis is employed to assess the dynamic phenomena taking place inside the piping system of the unit, which reproduces the real layout of the plant. Each element is then discretized in multiple parts and, for each sub-volumes, the Navier Stokes equations are solved through an implicit integrating method. 1D analysis are employed also for the analysis of Heat Recovery Vapor Generator (HRVG) and condenser which are represented as a combination of flow volume and thermal masses discretized on turns in sub-elements.

Heat exchangers are modelled through a Main-Secondary approach. For the HRVG, Main section reproduce the thermal power exchange between the HRVG metallic masses and the working fluid (R245fa), while Secondary one between exhaust gases and metallic masses. Concerning condenser, the Main models the thermal power exchange between the working fluid and the metallic masses, whereas the Secondary considers the thermal power provided by the metallic mass to the cold source (tap water). The model allows to consider the effect of thermal inertia of the HRVG and condenser metallic masses and the conductive capacity, allowing to perform a dynamic evaluation (equation (1); the wall temperature T_{wall} can be evaluated according to the thermal power balance between the heat exchanger and the two fluids.

$$\frac{dT_{wall}}{dt} = \frac{Q_1 + Q_2}{\rho V c_p} = \frac{(uA\Delta T)_1 + (uA\Delta T)_2}{\rho V c_p} \tag{1}$$

In equation (1), Q_1 and Q_2 are respectively the thermal power provided by the hot fluid to the metallic masses (positive sign) and thermal power provided by the metallic masses to the cold fluid (negative sign). ρ, V and c_p represent instead the density, volume and specific thermal capacity of metallic masses, respectively. Again, T_{wall} is the temperature of the metallic masses, t is the time independent variable and *h* is the heat transfer coefficient given in [W/m^2K].

Concerning the pump, it was modelled through a 0D approach based on equation (2), which allows to define the mass flow rate delivered. It depends on the pump rotational speed ω_{pmp}, the inlet fluid density $\rho_{pmp,in}$ and the displacement V_{disp} of the machine, considering a proper volumetric efficiency η_{vol}.

$$\dot{m}_{WF} = \omega_{pmp,FF}\rho_{pmp,in}V_{disp}\eta_{vol} \tag{2}$$

The power absorption is instead evaluated according to experimentally derived relation. For the expander, a look-up table built thanks to the wide experimental database was adopted, which allows to achieve a high rate of fidelity in the reproduction of experimental results [36] and low computational time and effort.

Concerning the boundary conditions, the following quantities are considered:

A. Exhaust gases mass flow rate and inlet temperature at HRVG inlet.
B. Exhaust gases pressure at HRVG outlet.
C. Pump speed which, according to equation (2), defines the mass flow rate flowing inside the plant
D. Cold water pressure at condenser outlet
E. Cold water mass flow rate and temperature at condenser inlet
F. Expander speed. The adopted subroutine allows to evaluate the expander speed as function of pressure difference between the expander intake and exhaust pressure. Indeed, for the adopted architecture the expander speed is not externally imposed but depends on the dynamic equilibrium on the machine shaft. It was seen in [37] that a linear dependence exists between expander pressure difference and its speed. Subroutine F in Fig. 2 reproduces this relation.

Further information about the model can be found in [37]. The main novelty introduced on the model is the development of dedicated subroutine allowing to reproduce the impact of the regulating system on the whole ORC-based unit property. The regulating system is composed by the integration of a Feedforward and a Feedback section. In the next section, the detailed scheme of this control system is deeply described.

2.3. 2.3.Feed Forward (FF) and feedback (FDB) control strategy

The adopted control strategy is based on the integration of a Feedforward (FF) and Feedback (FDB) regulating approach. Both strategies concur to provide the pump speed setting a working fluid mass flow rate, which ensures to achieve a superheating degree at expander inlet close to a value of 10 °C, and avoiding that temperature higher than 160 °C was reached, being this value an operating limit for the fluid and the components. A superheating degree equals to 10 °C is chosen as experimental and theoretical analyses confirm that this value maximizes expander performance [20,22]. Considering the case at hand, the only regulating parameter is the pump speed as the expander speed is not externally controllable.

The regulating strategy is shown in Fig. 3, where the following main step can be recognized.

1 The actual expander intake pressure is sensed evaluating the enthalpy corresponding to this pressure value and a superheating of 10 °C (eq. (3).

$$h_{hrvg,out} = h\left(p_{exp,in}, \Delta T_{SH}\right) \tag{3}$$

2 Sensing the pressure and temperature at evaporator inlet, the corresponding enthalpy value is evaluated (eq. (4).

$$h_{hrvg,in} = h\left(p_{hrvg,in}, T_{hrvg,in}\right) \tag{4}$$

3 Collecting the exhaust gas mass flow rate and their temperature at HRVG inlet and outlet, the actual recovered thermal power is calculated (eq. (5).

$$Q_{rec} = \dot{m}_{exh,gas}c_{p,exh,gas}\left(T_{hrvg,in} - T_{hrvg,out}\right) \tag{5}$$

4 Once the previous step is completed, the working fluid mass flow rate required is found (eq. (6).

$$\dot{m}_{WF} = \frac{Q_{rec}}{\left(h_{hrvg,out} - h_{hrvg,in}\right)} \tag{6}$$

5 As the pump is a volumetric machine, the pump speed needed to guarantee the working fluid mass flow rate known from step 4 can be assessed as follows (eq.7).

$$\omega_{pmp,FF} = \frac{\dot{m}_{WF}}{\rho_{pmp,in}V_{disp}\eta_{vol}} \rightarrow \omega_{pmp,FF} = k_{m\omega}\dot{m}_{WF} \tag{7}$$

The value of pump speed provided by feedforward section act as base value which is subsequently refined through the feedback section according to the following step:

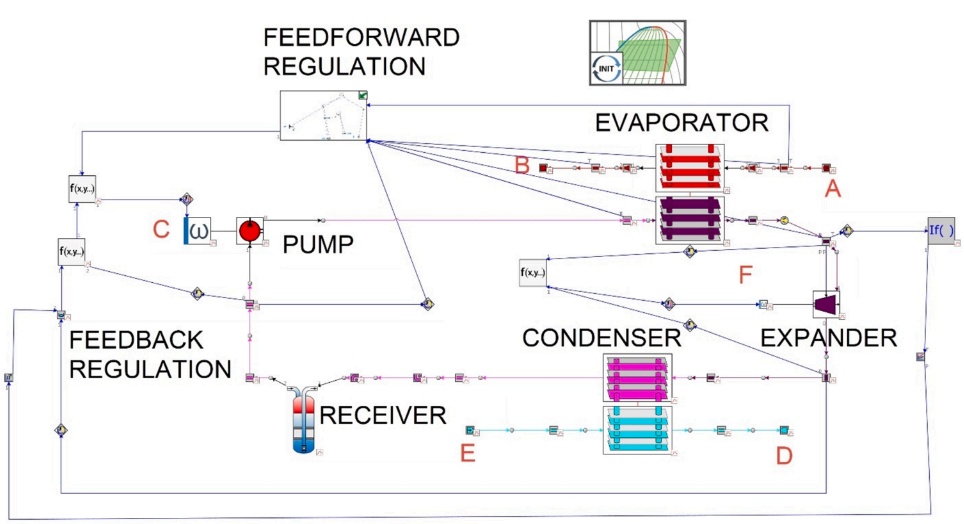

Fig. 2. Scheme of the 0D-1D comprehensive model of the unit.

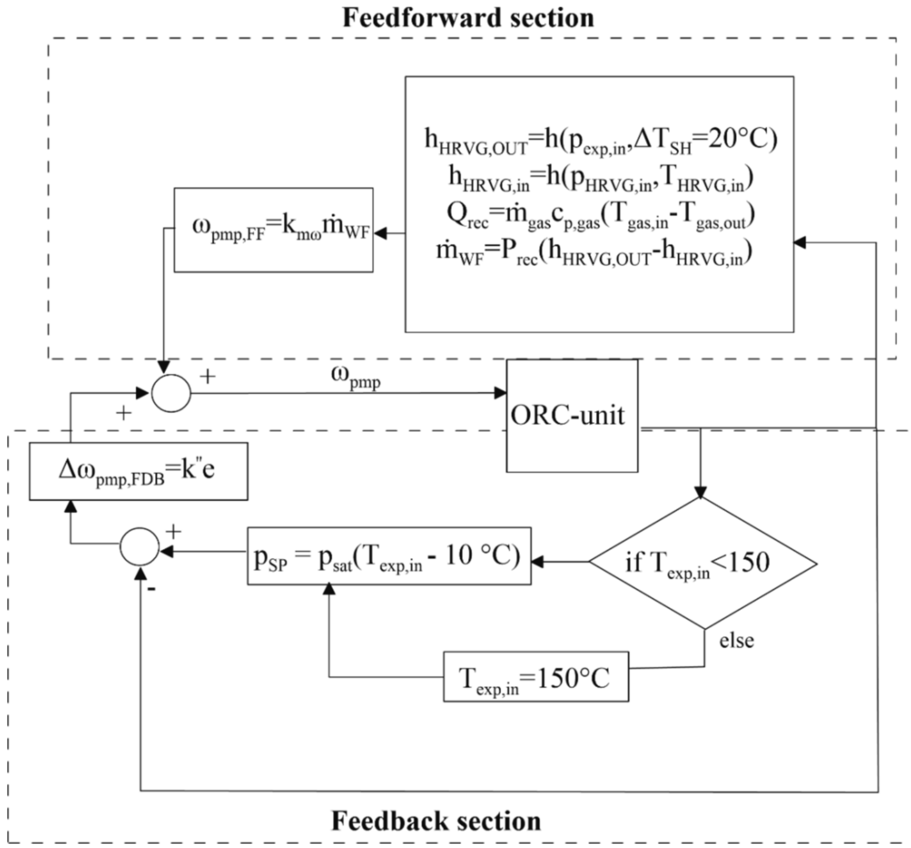

Fig. 3. Control strategy based on the integration between feedback and feedforward regulating strategy.

1 The expander intake temperature is sensed. If this value is lower than 150 °C, the pressure corresponding to the case in which the working fluid has a temperature equal to the sensed expander intake temperature and a superheating degree of 10 °C is evaluated. Otherwise, the pressure corresponding to the case in which the temperature is 150 °C and the superheating degree is 10 °C is calculated. This pressure value represents the Set point SP of regulating strategy (eq. (8).

$$p_{SP} = T_{sat}\left(T_{exp,in} - 10^{\circ}C\right) \tag{8}$$

2 Hence, comparing the SP with the actual value of pressure at expander intake, the error enters the proportional regulating section. The proportional gain k'' is evaluated thanks to the intrinsic linear relationship occurring between working fluid mass flow rate and expander intake pressure. Indeed, as authors widely observed in previous work [36,37] when volumetric expanders are used, the expander intake pressure assumes a quite linear growth with mass flow rate even if the speed is not externally set but is demanded to dynamic equilibrium on the expander shaft.

The slope is defined by the machine permeability expressed as the attitude of the expander to be crossed by the working fluid, [38]. Hence, the lower is the permeability the higher is the slope meaning that also small mass flow rate cause high expander intake pressure. This is clear considering that expander can be considered as revolving valve. Anyway, exploiting this concept, a physical proportional relation between mass flow rate and expander intake pressure can be derived. This allows to set the gain thank to a physical relation between the involved quantities avoiding to tuning this parameter. This is the main novelty introduced by the present work.

Hence, considering this proportional relationship, the eq. (9) can be written.

$$p_{exp,int} = k\dot{m}_{WF} + q \tag{9}$$

So, considering the difference between SP and actual pressure, the eq. (10) applies.

$$e = p_{SP} - p_{actual} = \left(k\dot{m}_{WF} + q\right)_{SP} - \left(k\dot{m}_{WF} + q\right)_{actual} = k\,\Delta\dot{m}_{WF} \tag{10}$$

Rearranging equation (9), equation (10) can be written expressing the relation between the error in terms of pressure (SP and actual) and the corresponding proportional variation of mass flow rate.

$$\Delta\dot{m}_{WF} = k' e \tag{11}$$

Where k' is the reciprocal of the slope (k) of the linear relationship between expander intake pressure and the mass flow rate (Fig. 4a). For the case at hand k and k' are equal to 153.07 [bar/kg/s] and 0.0065 [kg/s/bar], respectively.

Considering the proportional relation between mass flow rate and revolution speed, equation (2) and equation (11) can be combined thus expressing the proportional regulating action on the pump speed (eq.12).

$$\Delta\omega_{pmp,FDB} = k''e = \frac{k'}{\rho_{pmp,in}V_{disp}\eta_{vol}}e \tag{12}$$

Hence, the feedback section provides a refinement of the pump speed value set by feedforward section as equation (13) shows.

$$\omega_{pmp} = \omega_{pmp,FF} + \Delta\omega_{pmp,FDB} \tag{13}$$

It is important to observe that a permanent regime error is expected due the adoption of a proportional regulation without the integrative section. Moreover, the static feedforward approach neglects the dynamic effect at evaporator. Anyway, as aforementioned, the main goal of the present work is to develop a simplified regulating strategy allowing to ensure that main operating quantities are in safe range, rather than

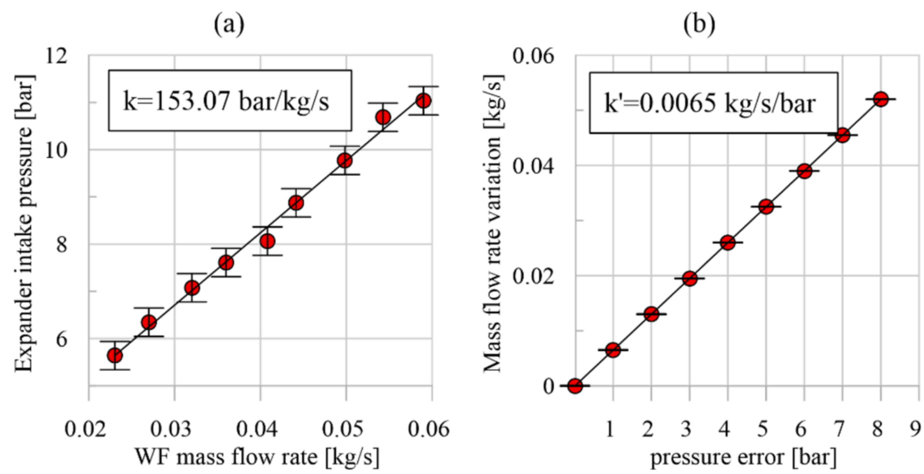

Fig. 4. Experimental expander intake pressure as function of mass flow rate (a) and mass flow rate variation as function of pressure error (b).

they assume specific value. The next results demonstrate that despite a regime error is observed, the plant can properly operate over severe heat source variations.

3. Results

3.1. Experimental validation

In order to experimentally validate the theoretical model of the whole ORC-based unit and find the intrinsic relation between the main operating quantities, a wide experimental analysis carried out. The ORC-based unit dynamic response to a step-variation of ICE speed (Fig. 5a), keeping its torque close to a value of 100 Nm, was firstly observed. The ICE speed step-variation leads to a proportional step-increase of exhaust gases mass flow rate and a first-order dynamic growth of exhaust gases from 280 °C up to 340 °C (Fig. 5b). In all measurements the grey area represents the uncertainty range.

As a consequence, the temperature of working fluid at expander intake, sees a slight proportional increase in correspondence to the variation of exhaust gases mass flow rate. This is followed by a typical first order dynamical growth (Fig. 6(a)).

Concerning the expander intake pressure (Fig. 6b), it is slightly affected by the ICE exhaust mass flow rate variation as the working fluid mass flow rate is kept constant to 0.04 kg/s. Indeed, for what observed in [36,37], working fluid mass flow rate is the main driver of the expander intake pressure growth. In this case, a slight first order dynamic increase is observed from 6.5 bar up to 7.1 bar.

Both expander intake pressure and temperature are accurately predicted as confirms the good agreement between the experimental and theoretical data reported in Fig. 6 (a) and (b). This is confirmed by the low Root Mean Square Error in absolute (RMSE) and relative form (RMSEr) evaluated as in eq.14.1 and 14.2:

$$RMSE = \sqrt{\frac{\sum_{i=1}^{N}\left(x_{p,i} - x_{s,i}\right)^2}{N}} \tag{14.1}$$

$$RMSEr = \sqrt{\frac{\sum_{i=1}^{N}\left(\frac{x_{p,i}-x_{s,i}}{x_{s,i}}\right)^2}{N}} \tag{14.2}$$

Where $x_{p,i}$ and $x_{s,I}$ are respectively the experimental and predicted quantities and N is the number of the experimental data.

Standard deviation (SD) of experimental measurement was also evaluated according to equation (14.3):

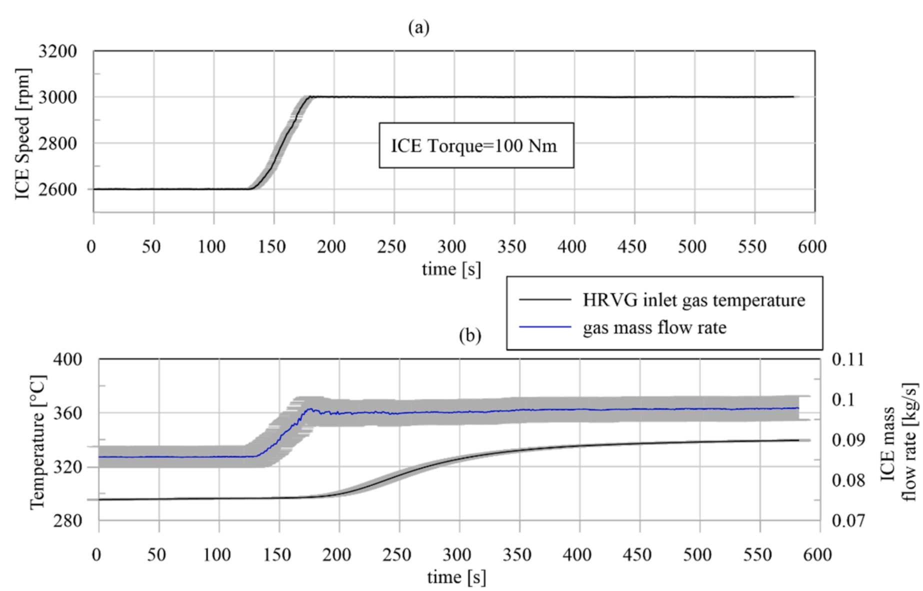

Fig. 5. ICE Speed (a), exhaust gas temperature (b) and mass flow rate (c) as function of time. Grey area represents the uncertainty range.

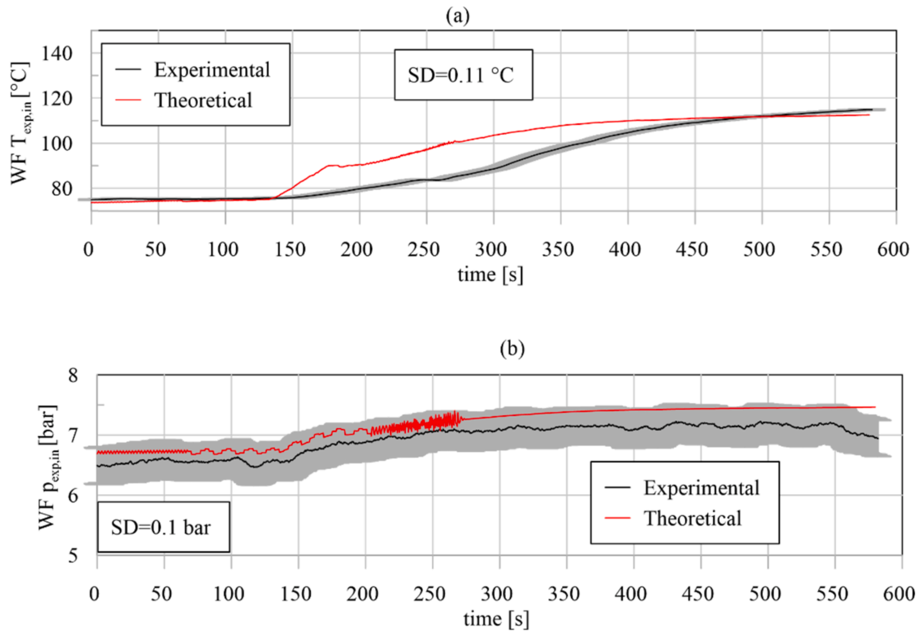

Fig. 6. Expander intake temperature (a) and pressure (b) as function of time.

$$SD = \sqrt{\frac{1}{N}\sum_{i=1}^{N}(x_i - \tau)} \tag{14.3}$$

where N is the number of the experimental values, xi is the i-experimental data and τ is the mean of the population.

Indeed, RMSE in terms of temperature (eq.14.1) and RMSEr in terms of pressure (eq.14.2) are respectively equal to 12.6 °C and 3.4 %. The same accuracy is encountered for expander and ORC-unit power shown in Fig. 7(a) and 7(b) respectively. It can be observed the good matching between theoretical and experimental data also for these quantities, confirmed by RMSEr (eq.14.2) equal to 5.4 % and 6.1 % respectively.

Errors are evaluated comparing the predicted data with the experimental ones for each i-time step being the model evaluating the dynamic response of the ORC-based power unit. Hence, Root Mean Square Error in absolute (RMSE) and relative (RMSEr) refers to the population of experimental and theoretical data representing the time evolution of a given quantity.

Observing the results, it can be seen that for pressure an RMSEr is equal to 3.6 % which is a good value considering that it corresponds to a deviation lower than the measurement uncertainty. This is shown also graphically by Fig. 6 in which it can be seen that the theoretical data are within the uncertainty bar (grey area).

As far as the temperature is concerned, the agreement is really accurate in correspondence to initial and final steady state as confirmed by Fig. 6(a) where it can be seen as theoretical prediction is within the uncertainty range. Moreover, also the time in which the final steady state value is accurately predicted. The accuracy is lower for the temperature prediction between 150 and 200 s in correspondence to which the model predicts a higher temperature increase in correspondence to the exiting cause (the exhaust gas mass flow rate increase). This is due to the unavoidable simplification of HRVG geometry and discretization which cannot be over-refined in order to avoid large computation time. The RMSE is affected by the errors in this region, anyway, it is not affect

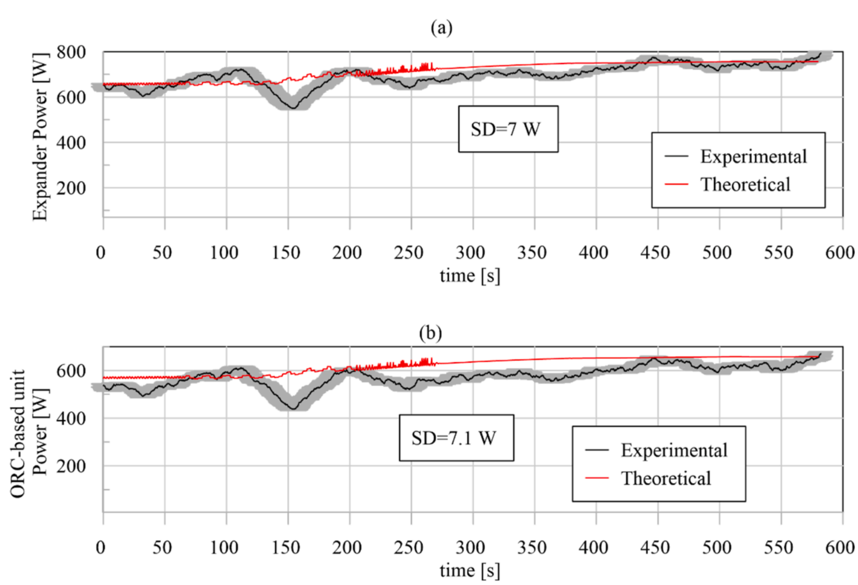

Fig. 7. Expander (a) and ORC-plant power (b) as function of time.

the real feature of the model to accurately predict the final value and the time needed to achieve it.

Therefore, it was demonstrated the capability of the model to represent the dynamic behaviour of the main ORC operating quantities (expander intake pressure and temperature) and the main output (expander and ORC-plant power) in response to a dynamic variation of the boundary conditions. This makes reliable the prediction of the effect introduced by the proposed regulating strategy on the ORC-based power unit behaviour.

As aforementioned, in this case the variation of ICE operating conditions does not produce a significant modification of expander intake pressure. Indeed, the main driver of expander intake pressure variation is due to the variation of working fluid mass flow rate, [39]. What is more, such relation can be retained linear or sub-linear (Fig. 4). This leads to a quasi-steady variation as it can be observed from Fig. 8.1 by the instantaneous variation of the pressure in response to a mass flow rate step change.

Fig. 8.1 is related to the case where the ICE operating conditions are fixed (ICE torque equal to 100 Nm and ICE speed of 3000 rpm). A step-change of working fluid mass flow rate from 0.04 kg/s and 0.06 kg/s occurs leading to an over oscillation of expander intake pressure from 7 up to 9 bar. Such over oscillation expires after 50 s when a constant values 7.8 bar is established. Hence, given this short period of time, the variation of expander intake pressure can be retained proportional to the mass flow rate. This means that the variation of working fluid mass flow rate (which suddenly follows the pump speed regulation) allows to provide a proportional effect on the expander intake pressure which is the base of the proposed regulating strategy. In this way, a fast-regulating action on the expander intake pressure can be provided. It is particularly suitable since the high fluctuation of the operating condition. Despite the expander intake temperature sees a first-order dynamic variation (decrease in this case) after 70 s the novel steady state is reached. This reinforces the effectiveness of the regulating strategy based on the working fluid mass flow rate to control the working fluid condition at expander intake.

It is important to observe that the same behaviour is observed when a sudden decrease takes place (Fig. 8.2). In this case, consequently to the step decrease of mass flow rate, the pressure decreases after a slight over-oscillation expiring after 50 s and also in this case, due to the lower overshoot time duration the relation between expander intake pressure and mass flow rate can be retained quasi-steady. In other words, the dynamic of the expander can be retained negligible to that to evaporator as demonstrated by the first-order dynamic variation of the temperature in response to mass flow rate step variation.

Considering the step variation of the working fluid mass flow rate (case in Fig. 8.1), the pressure and temperature at the discharge and suction sides of the pump was reported in Figure 8.3(a) and (b) respectively. It can be seen that the pump outlet pressure sees a proportional increase with the mass flow rate variation, Considering the temperature at pump sides the are closer as can be theoretically expected. In Figure 8.4(a) the expander and pump power are reported. It can be observed that both device sees a rapid variation with working fluid mass flow rate step-change. In particular the expander power decrease because the increase of pressure and the decrease of temperature of the working fluid at expander intake leads to a diminution of superheating degree at expander intake thus decreasing the machine efficiency (Fig. 8.4 (b)). In order to avoid that after pump speed step increase the superheating decrease excessively (up to case in which the complete vaporization cannot be ensured) the superheating degree at the start of the test was intentionally taken high (50 °C) as it can be seen from the absolute entropy diagram of the cycle on which ORC-based power unit is based(Fig. 8.5).

This necessity involves that a low working fluid mass flow rate should be kept (0.04 kg/s) in order to guarantee proper superheating degree. Indeed, the lower is the working fluid mass flow rate the lower is the evaporating pressure for the permeability theory [36,37]. This choice is taken exclusively to provide safe dynamic test thus stressing the increase of pump speed and consequently the decrease of expander intake temperature (and superheating degree respectively). Indeed, increasing the working fluid mass flow rate the ORC-plant performance increases significantly as the expander intake pressure increase as observed in authors previous work, [40].

It is also worth to notice that the data are experimentally-based ones, both exhaust temperatures, ORC temperatures and pressure, ORC net power. The large pinch point observed is the result of the thermal equilibrium reached in the evaporator, considering the limits of a real experimental unit: a) the fluid temperature cannot overcame 160 °C to avoid thermal degradation of the fluid itself; b) the inlet temperature of an expander should be also limited, to reduce the thermal distortions of materials and avoid breaking of the sub-components; c) evaporating pressure should be limited to 25–30 bar to preserve the integrity of the sealing component of the expander; d) the mass flow rate is not independent from the evaporating pressure, but it is related to the permeability of the ORC circuit.

Moreover, the large pinch point temperature among the exhaust gases and the organic fluid consented to design a compact evaporator,

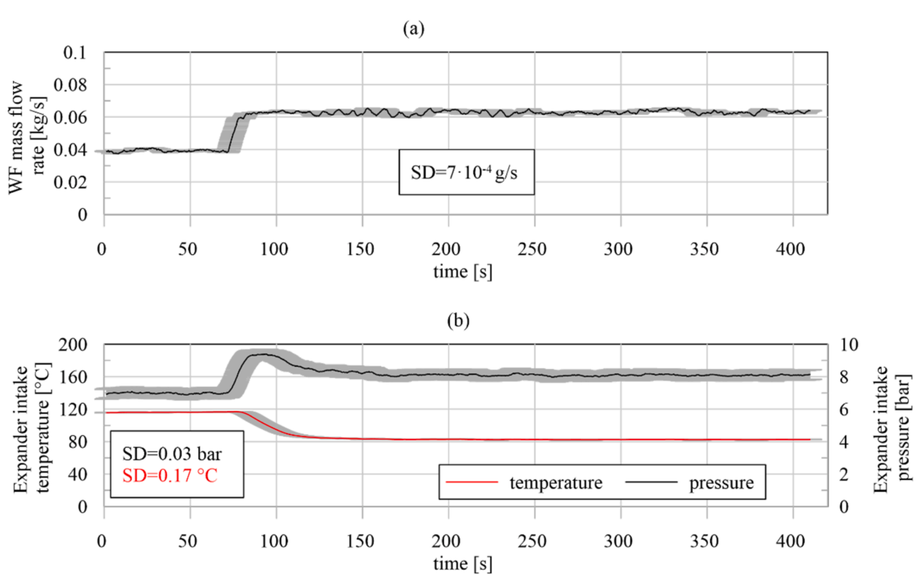

Fig. 8.1. Positive WF mass flow rate step increase (a) and its effects on expander intake temperature and pressure (b).

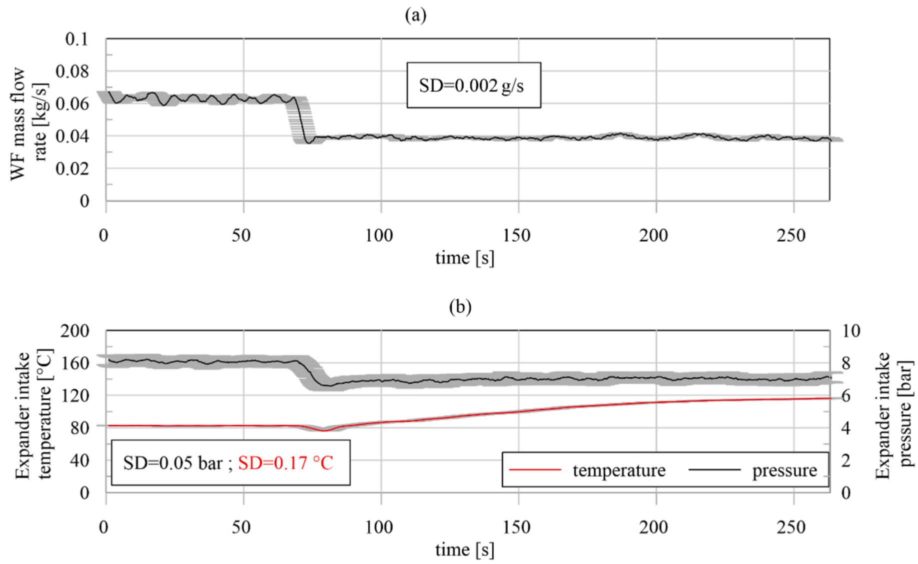

Fig. 8.2. Negative WF mass flow rate step increase (a) and its effects on expander intake temperature and pressure (b).

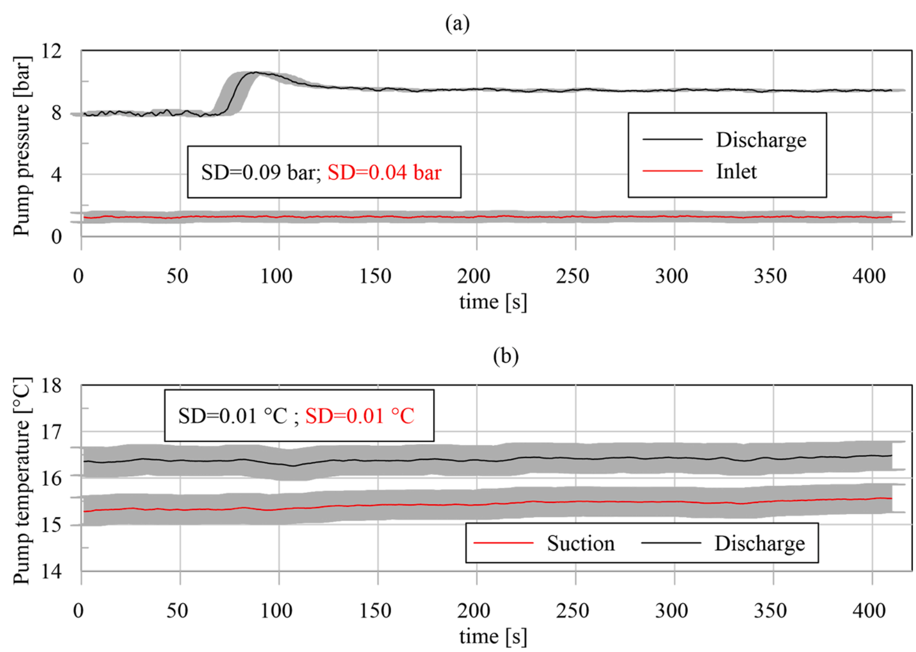

Fig. 8.3. Pump discharge and suction pressure (a) temperature (b).

according to equation (15),[41]:

$$Q = U{\cdot}A{\cdot}LMDT \tag{15}$$

Where A is the heat exchanger area, U is the heat transfer coefficient and LMDT is the Logarithmic mean temperature difference. This is a very important aspect in vehicle applications, since room in the vehicle is very limited and compact components are appreciated.

A second aspect is related to the power produced by the unit. Indeed, the power experimentally produced and then modeled is lower than the thermodynamic expectation, since it is evaluated at the end of the conversion chain, in DC electrical form. Indeed, the power reported in the paper comprises the thermodynamic efficiency of the machines, the mechanical conversion and the electrical efficiencies of both expander and pump (Fig. 8.4 (b)). Hence, the value is the net electrical value obtained from the validated model and, so, by the experimental unit tested at lab scale. Many experimental evidences confirm that real power recoverable from ICE exhaust is not more 2–3 % of the ICE mechanical power and a net plant efficiency is really lower than the thermodynamic one, [42,43].

Despite the quantities of Figs. 8.3 and 8.4 are not reported for the step-decrease case for the sake of brevity, also in this case a proportional relation between working fluid mass flow rate and plant maximum pressure were observed.

Authors provide a deep experimental analysis on the dynamic behaviour of ORC-based power unit subjected to step-variation of ICE torque and speed or working fluid pump mass flow rate.

After a significant number of experimental tests, a repeatability analysis was carried out confirming that:

a) ICE speed step increase keeping constant ICE torque and working fluid pump speed. As a consequence the exhaust gases mass flow rate sees a sudden increase due to the fact that the speed increase

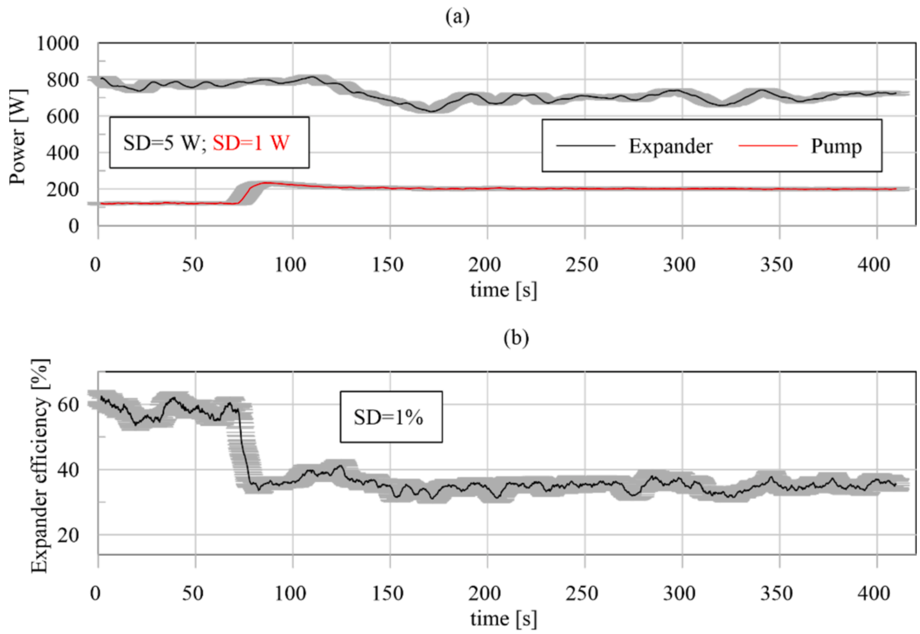

Fig. 8.4. Expander and pump power (a) and efficiency (b).

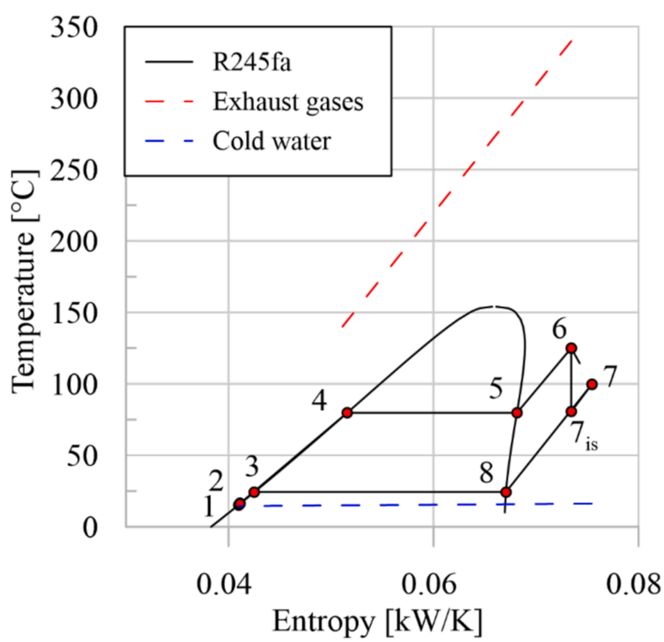

Fig. 8.5. Absolute entropy diagram of the ORC-based power unit in correspondence of the steady state before pump speed step change of Fig. 8.1.

produces higher ICE cycles and consequently a larger exhaust gases mass flow rate. Also the exhaust gases temperature performs a first order dynamic growth caused by the enhancement of the engine load. The expander intake pressure follows a slight first order dynamic growth due to the increase of superheating degree at expander intake side. Such observation are in accordance to that performed by the authors in [36] where the ORC-dynamic response to ICE speed step variation was observed;

b) Also the ORC-dynamic response to step variation of pump speed is in accordance with previous experimental results collected by the authors in [39]. Indeed, it was noticed that if the ICE torque and speed are kept constant, the pump speed increase produces a proportional growth of the expander intake pressure due to the expander permeability theory, [36] on which the current regulating procedure is based. Therefore, as the exhaust gases mass flow rate and temperature at HRVG inlet are constant (ICE operating point was not varied) the increase of working fluid mass flow rate leads to a decrease of temperature of working fluid at the HRVG outlet (and expander inlet).

3.2. Assessment of benefits introduced by plant regulation

Once the model was experimentally validated, it was used to predict the positive impact of the proposed regulating strategy on the plant behaviour. Such analysis is fundamental to assess the validity of a control strategy prior to implement it on board and to develop complex electronic boards. Such approach is widely adopted in literature, where control strategies were preliminary tested thanks to physical model of the unit [17,42].

The first analysis was carried out comparing the baseline case with that in which the control strategy was employed. The ORC dynamic behaviour was evaluated in response to a combined forcing cause given by a step variation of exhaust gases mass flow rate and a first order dynamic growth of exhaust gases inlet temperature (Fig. 9(a)). These variations of exhaust gases properties are due to a step variation of ICE speed not reported for the sake of simplicity in the figure being similar to that of Fig. 5).

In Fig. 9(b), the time evolution of working fluid temperature at expander inlet is reported in the regulated FF-FDB and baseline case, without control. In the baseline case, the working fluid inlet temperature follows the typical first-order growth reaching temperature of 180 °C beyond the maximum limit allowed for the machine component integrity (160 °C). Hence, unsafe and unsuitable working conditions are encountered in baseline conditions. On the contrary, with the ORC-based unit regulated through a FF-FDB strategy (Fig. 9(b)) it was achieved a temperature equal to 130 °C at the steady state reached after 150 s from the step variation of exhaust gas mass flow rate (and consequently of the ICE speed). Moreover, despite an overshoot of the order of ± 20 K are observed during the transient period, they are always lower than the operating limit. It is worth to notice that, in the present analysis, the baseline and regulated ORC plant are at ambient conditions when the test starts. This justifies the sudden variation of temperature.

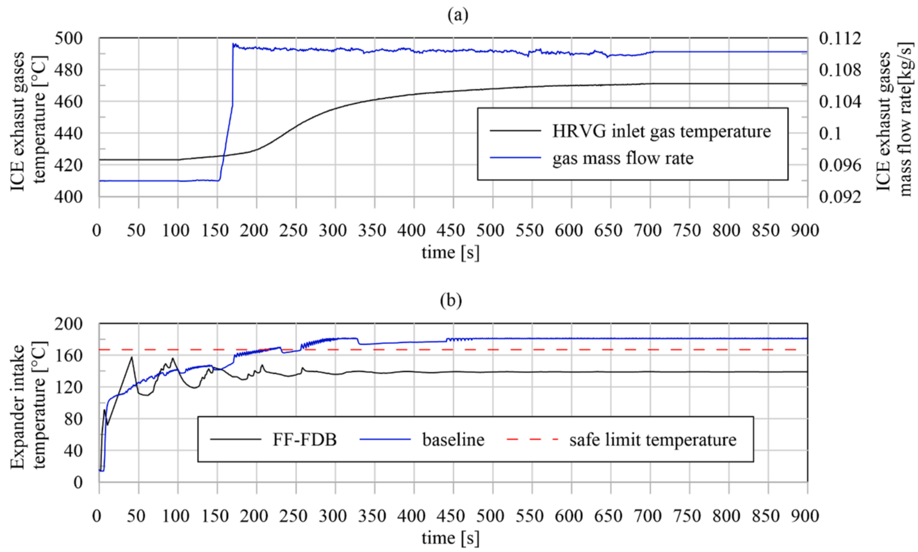

Fig. 9. Exhaust gases temperature and mass flow rate (a) and expander intake temperature and pressure (b) as a function in case of regulated FF-FDB and baseline ORC-unit (b) over time.

For what concerns the expander intake pressure, comparable values are achieved in the case of regulated and baseline systems as it can be seen in Fig. 10. Hence, the lower temperature at expander intake in the regulated case, allows to reduce the superheating degree with respect to the baseline case (Fig. 11(a)). Indeed, if the system is regulated the plant reach the steady state value after 300 s with a superheating degree of 20 °C. It is important to remark that the large time to achieve the steady state is due to the dynamic growth of the exhaust gases temperature (caused by the thermal inertia of the metallic masses connecting the ICEs to the evaporator and by the thermal inertia of HRVG metallic masses [36]. Therefore, it is not a responsibility of the proposed regulating strategy which, anyway, presents a rapid adaptation of the fluctuant heat source, damping its variation as well. Despite a regime error of 10 °C is observed with respect to the desired set point (10 °C), the actual superheating value (20 °C) is still in the optimal range for a good operation of the plant. Indeed, the target is ensured since operating quantities are in a prescribed range. Indeed, the ORC-based power unit can provide good performance even if the superheating degree at expander intake varies in a range between 5 and 30 °C. In this way, satisfying performance, safe operation and low computational cost can be obtained.

Hence, benefits pursued with respect to the baseline case are clear. Indeed, the steady state superheating degree is equal to 60 °C (Fig. 11 (a)). The superheating degree should be limited to avoid problem related to the chemical decomposition of the working fluid [43], which for R245fa is equal to 440 K [44]. Moreover, the proposed regulating system allows to avoid that superheating degree exceeds 40 °C during the transient period. Indeed, in this timeframe overshot of −10 K/30 K (typical of FDB strategies) is observed around the set point value of 10 °C, whose amplitude diminishes as the steady state point is approaching. Anyway, the behaviour of regulating system during the transient phase is particularly important. Indeed, in the real application, the ICE operating point changes frequently without the possibility to the unit to reach the corresponding steady state. Therefore, the capability of the system to avoid over excursion of working fluid is fundamental to prevent problem related to the working fluid decomposition. Similarly, the superheating degree should be kept at least few degrees higher than 0, in order to exclude the situation in which a two-phase working fluid is elaborated by the machine. Anyway, this latter situation is less dangerous than the previous as the machine is able to work with a little part of two-phase working fluid.

The control of superheating degree is achieved thanks to the control of working fluid mass flow rate provided by the pump. Indeed, in Fig. 11 (b) it can be recognized the integrated effect of feedforward and feedback regulating section. The FF section allows to set an initial value according to the thermal power equilibrium at HRVG, whereas the FDB section ensures to refine the working fluid mass flow rate value exploiting the proportional relation between mass flow rate and expander intake pressure given by the expander permeability.

Indeed, it can be observed as the average value of working fluid mass flow rate grows following the increase of thermal power available at evaporator due to the FF regulating system. On the other hand, the oscillation caused by the effect of the FDB section reduces their amplitude as the steady state value is approached.

Hence, it can be concluded that thanks to the integrated action of FF (on the thermal power equilibrium at evaporator) and of the FDB section (on the maximum plant pressure) the desired superheating degree can be achieved avoiding over-excursion of working fluid temperature.

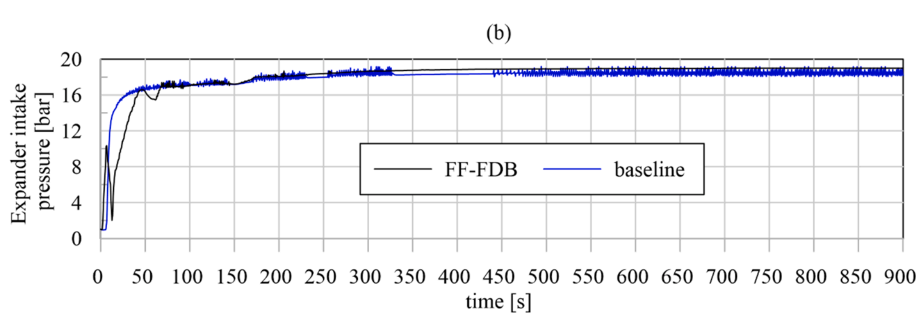

Fig. 10. Expander intake pressure as a function in case of regulated FF-FDB and baseline ORC-unit over time.

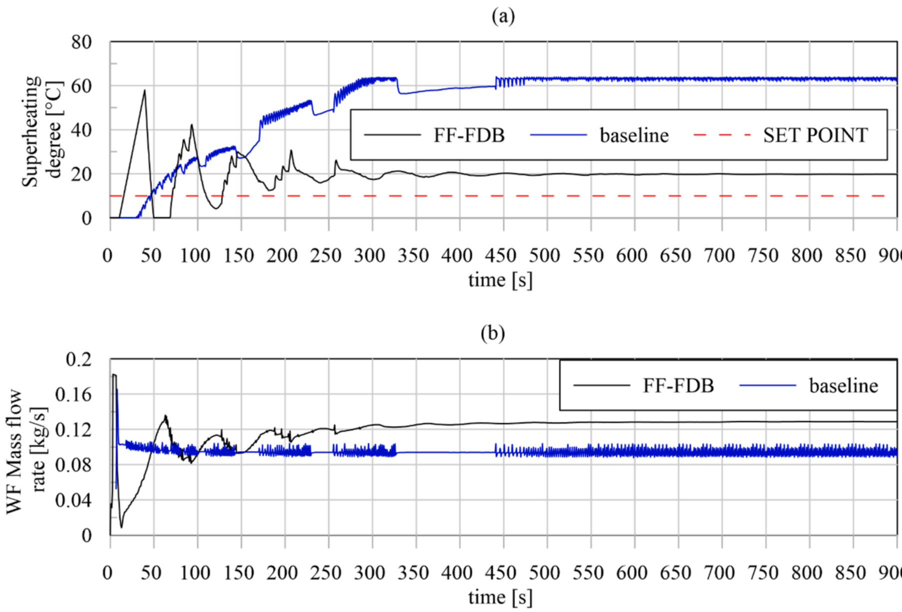

Fig. 11a. Superheating degree of working fluid at expander intake (a), WF mass flow rate (b) in case of regulated FF-FDB and baseline ORC-unit (b) over time.

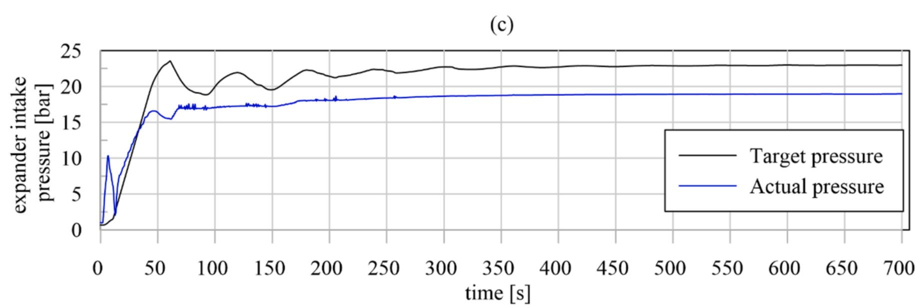

Fig. 11b. Target and actual value of expander intake pressure (c) in regulated FF-FDB ORC-unit over time.

As aforementioned, the FDB section adopts a proportional regulator approach, hence, a permanent regime error is expected on the controlled variable (expander intake pressure). Such error can be observed in Figure 11(c) where the difference between the target and actual pressure value can be noticed. Despite an error close to 18 % is observed, it does not affect the reliability of the regulating system as noticed in the previous picture keeping the operating quantities within the safe limits. Hence, the simplicity of the proposed strategy and the robustness provided to the system justify the permanent regime error observed. Moreover, the unit does not have the time to reach the steady state for a sudden and frequent variation of the ICE operating points, thus, this makes more important that the regulating system ensures to maintain the operating quantities in the prescribed range during the transient period. Anyway, the permanent regime error could be improved properly introducing an integrative section thus adopting a Proportional Integrative (PI) regulating system.

In Fig. 12, the performances of the regulated unit are reported in terms of expander and ORC-unit power (a) and plant efficiency (b). It can be observed as the expander power reaches a steady state value equal to 1.5 kW. However, even during the transient period the power production is significant achieving the production close to 1 kW after 100 s.

For what concerns the ORC-based unit power, it is equal to the difference between expander and pump power. Hence, the trend is the same of that of the expander but downshifted due to the pump power consumption which is significant (17 % of the expander power).

Concerning the efficiency, it is evaluated as the ratio between the ORC-based unit power and the thermal power of the exhaust gases provided to the system (eq.16):

$$\eta_{ORC} = \frac{P_{ORC}}{\dot{m}_{exh,gas} c_{p,exh,gas} \left(T_{exh,gas,in} - T_{exh,gas,out}\right)} \tag{16}$$

It can be observed from Fig. 12(b) that a steady state value of 4 % is achieved and a 3 % is reached only after 100 s. These results are in accordance with the best literature value for similar applications [44].

3.3. 3.4.Regulated ORC-unit over transient operating conditions

The previous comparison carried out for a single step-change of ICE operating condition allows to put in light the fundamental dynamic response of the unit in baseline and regulated cases. Anyway, to be closer to the real application, a sequence of heat source fluctuation should be considered. Indeed, in this case, for the continuous variation of the external cause, the system has lower time to reach the novel steady state conditions. Moreover, such conditions are harsher than the previous ones, allowing to better evaluate the positive impact of regulating system.

For all these reasons, a sequence of step changes is considered for gas temperature and mass flow rate [45]. The step changes last different timeframe to observe the response of regulated system to an irregular and aleatory heat source conditions variation. This can be noticed in Fig. 13(a), where the step-change trains for gases temperature and mass flow rate can be seen. The behaviour of the plant with the FF-FDB regulated system was analysed in response to this solicitation

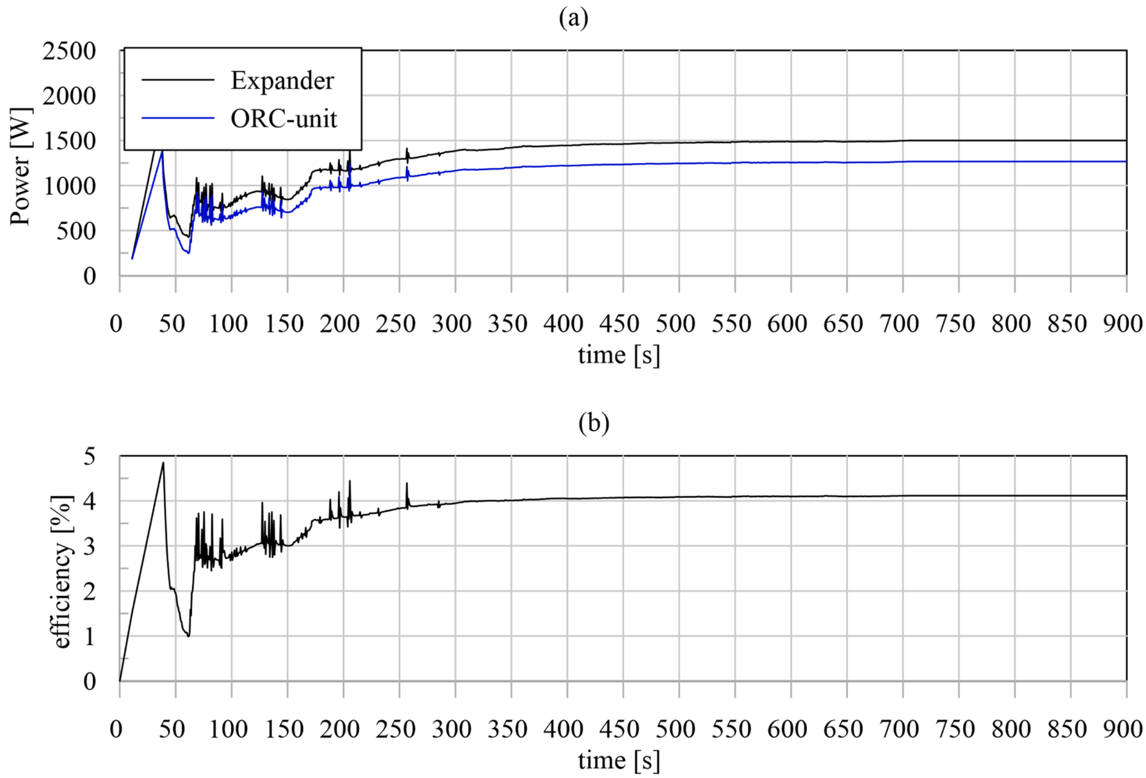

Fig. 12. Expander and ORC-unit power (a) and ORC-unit efficiency (b) in case of regulated FF-FDB regulation over time.

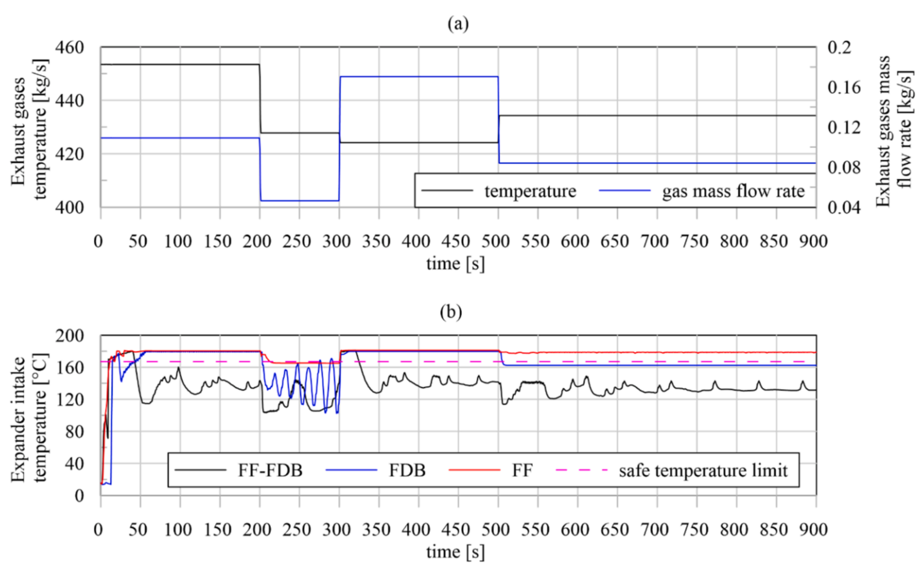

Fig. 13. Exhaust gases temperature and mass flow rate (a) and expander intake temperature (b) in case of FF-FDB, FDB and FF regulated ORC-unit over time.

sequence. Furthermore, to demonstrate the necessity of integration of FF-FDB, also the case in which only the FF and FDB regulations are considered separately [17].

In Fig. 13(b), the expander intake temperature in case of FF-FDB, FF and FDB approaches is reported respectively. It can be observed that only with the integration of the two action (FF-FDB) the temperature can be kept lower the limit of 160 °C which is given not only by the machine components integrity, but it is also due to the chemical decomposition temperature of R245fa. Hence, even if the adopted static FF strategy is relatively simple, its integration with a FDB section ensures to fully satisfy the regulating goal saving at same time computational cost and model complexity compatibly with the short time of heat source variation.

In Fig. 14, the reason of the benefits of the FF-FDB strategy can be seen. In fact, only the integration of the two section (FF and FDB) allows to provide the adequate level of working fluid mass flow rate which is significantly higher than that provided by the FF and FDB considered separately.

The better management of temperature (Fig. 13b) and pressure (Fig. 15b) leads to a superheating degree close to the desired value (10 °C). It is interesting to notice that even though the sequence of step variations, superheating degree are always kept lower than 40 °C. Hence, despite the short-time fluctuations of the heat source, the ORC conditions are quite stable and always within the safe range.

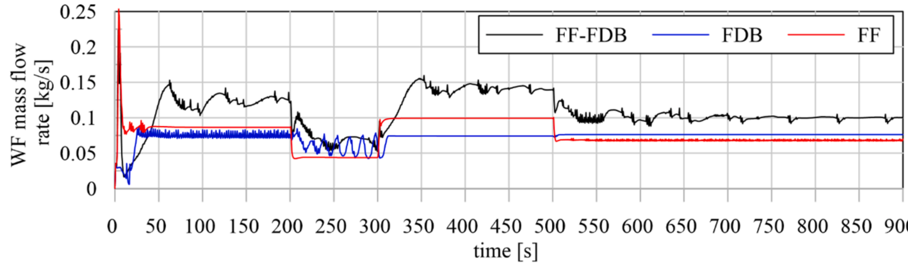

Fig. 14. WF Mass flow rate in case of FF-FDB, FDB and FF regulated ORC-unit over time.

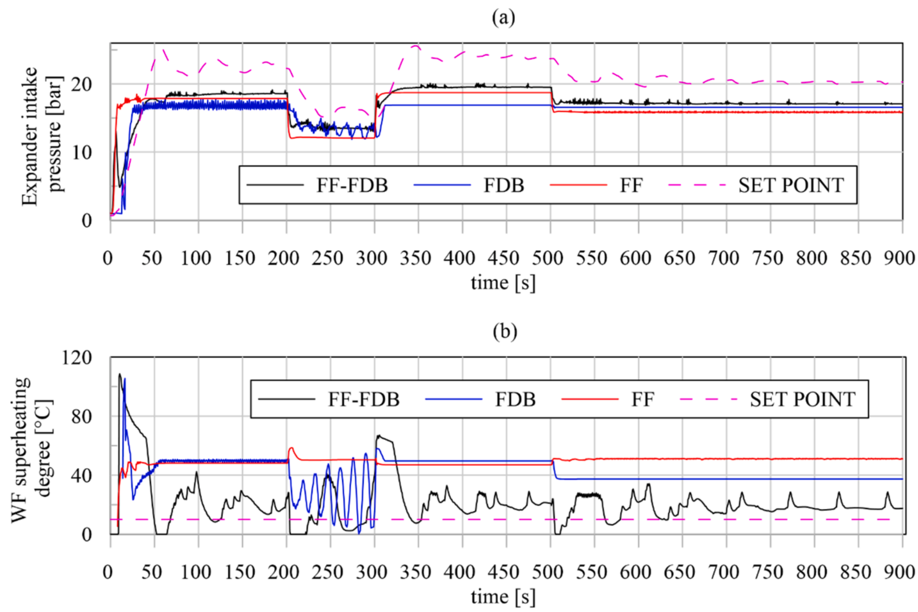

Fig. 15. Expander intake pressure (a) and WF superheating degree in case of FF-FDB, FDB and FF regulated ORC-unit over time.

The final result is related to the power output and the ORC global efficiency of FF-FDB case, Fig. 16. The system presents expander power ranging from 1 up to 2 kW with peaks of 3 kW. Moreover, despite the high fluctuation of the heat source, the produced power is relatively stable at step-change variation. For the aforementioned reason, the ORC-unit power has the same trend with a downward shift due to the

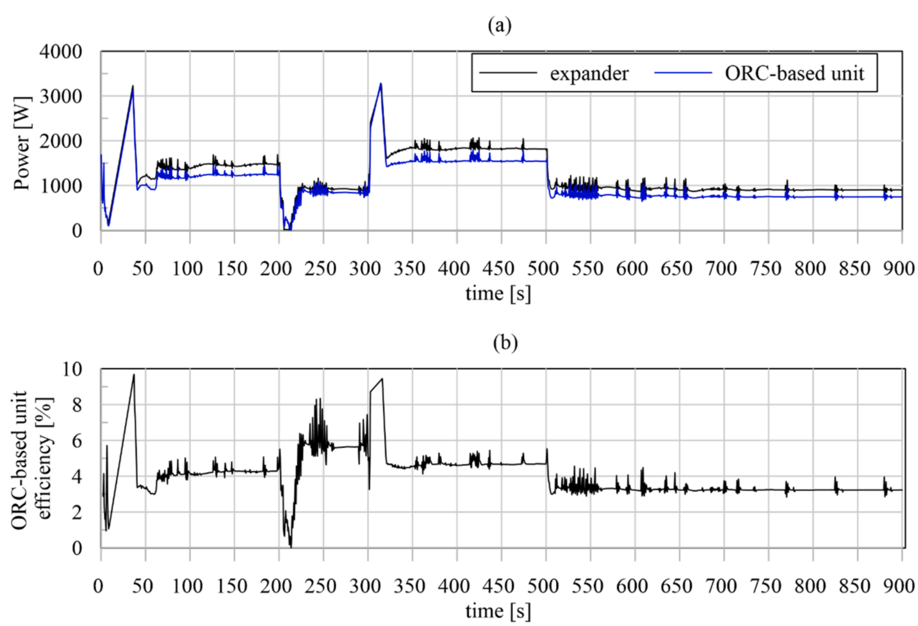

Fig. 16. Expander and ORC-based unit power (a), ORC-based unit efficiency (b) over time in FF-FDB case.

pump absorbed power.

The good performance in terms of power leads to the achievement of satisfying efficiency values. Indeed, these ranges from a minimum value of 4 % up to a maximum of 6 % with rare peaks up to 8 % (Fig. 16(b)).

Hence, the control strategy proposed perform better in terms of safety values reached, when the exhaust gases of the ICE changes their thermodynamic conditions and mass flow rate. These robustness in off-design conditions is the most important result. In terms of cycle efficiency, the values are not significantly changed. This can be demonstrated by the evaporating pressure in Fig. 15b, which is not significantly changed by the control strategies compared. A better management in superheating degree is also demonstrated. In terms of output power, the higher mass flow rate reported in Fig. 14 for FF-FDB strategy consents to have higher net power, with similar thermodynamic conditions.

The good performance demonstrated by the adoption of the proposed regulating system to the ORC-based power at hand paving the way for a diffusion in other sectors. Indeed, ORC-based power units fed by the exhaust gases of ICE are subjected to frequent and severe variation of the operating condition. Hence, if the regulating strategy works well, it can be adopted also in other application characterized by a variable hot source. This is the case, for example, with ORC-based power units employed in hybrid solar geothermal system and for all the case in which the hot source is characterized by inherent variability.

4. Conclusions

In the present paper, a regulating strategy for Organic Rankine Cycle (ORC)-based power unit fed by the exhaust gases of a 3 L Internal Combustion Engine was developed. The benefits introduced by the control system are assessed thanks to a comprehensive theoretical model of the whole unit allowing to reproduce its physical behaviour. The model reliability was demonstrated by the validation against a wide experimental data collected on a dedicated experimental test bench conceived to recover the thermal power of an Iveco F1C ICE. The experimental data are referred to dynamic conditions, hence, the predictions offered by the model ensures to reproduce with a high rate of fidelity the dynamic behaviour of the plant in response to fluctuation of the heat source. Indeed, Root Mean Square Error in terms of maximum plant pressure (RMSEr) and temperature (RMSE) are in the order of 3.4 % and 12.6 °C respectively. The RMSEr in terms of expander and net plant power output are instead respectively equal to 5 % and 6 %. This means that the model can catch the time evolution of the main regulating parameter (maximum pressure and temperature) and power output making highly reliable the assessment of the benefits introduced by the adoption of the regulating strategy.

The regulating strategy is based on the integration of a feedforward and a feedback section with proportional regulators. The novelty introduced by the proposed strategy is the FDB section, based on a constitutive relationship between expander intake pressure and working fluid mass flow rate (and consequently pump speed). Indeed, experimental analysis confirms that between expander intake pressure and mass flow rate a quite linear dependence takes place, whose slope is affected by the expander permeability, defined as the attitude of the machine to be crossed by working fluid. Hence, the gain of the proportional regulator can be evaluated as the slope of the working fluid mass flow rate linear variation as function of the expander intake pressure. Such aspect represents a significant novelty as this approach allows to avoid the parameter identification through mathematical tools generally adopted in literature. Thanks to this FDB section, even if the FF regulating part is significantly simple with respect to that based on predictive model, their integration allows to satisfy the functional requirements. In fact, if subjected to short-time variations of heat source, the adoption of the FF-FDB regulating strategy allows to:

- keep the temperature lower than the prescribed limit 160 °C, in order to avoid the chemical decomposition temperature of the R245fa (167 °C) and damage expander and other components;
- achieve a steady state value of superheating degree close to 15–20 °C, which is defined as the best operating condition.
- in real application, the achievement of steady state is not guaranteed due to the frequent variation of the heat source, so the unit could operate always in dynamic conditions. Anyway, it was seen that FF-FDB allows to avoid that over and under oscillations around the set point (10 °C) exceed values higher than 40 °C.
- despite the heat source variation, the plant is able to provide continuously an ORC-based unit net power ranging from 1 and 2 kW with an efficiency between 4 and 6 %, excluding occasionally peaks up to 8 %;
- if considered separately, FF and FBD section does not satisfy the requirements due to the simplicity of regulations;
- as theoretically expected, the adoption of a proportional regulator introduces a regime permanent error which does not affect the reliability of the system, and can be improved introducing an integrative section in the regulator.

Finally, the control approach presented ensures that operating quantities are in a prescribed range, granting safety and flexibility at the same time. This involves a significant computational time and cost saving, but without affecting the performance level of the ORC-based unit.

Declaration of competing interest

The authors declare that they have no known competing financial interests or personal relationships that could have appeared to influence the work reported in this paper.

Data availability

Data will be made available on request.

References

[1] https://ourworldindata.org/ghg-emissions-by-sector.
[2] https://www.consilium.europa.eu/en/policies/green-deal/.
[3] Gustavo Adolfo Gómez-Ramírez, Rebeca Solis-Ortega, Luis Alberto Ross-Lépiz, Impact of electric vechicles on power transmission grids, Heliyon, Volume 9, Issue 11, 2023, e22253, ISSN 2405-8440, https://doi.org/10.1016/j.heliyon.2023.e22253.
[4] Rafael Lago Sari, Alvaro Fogue Robles, Javier Monsalve Serrano, David Cleary, Techno-economic assessment of hydrogen as a fuel for internal combustion engines and proton exchange membrane fuel cells on long haul applications, Energy Conversion and Management, Volume 311, 2024, 118522, ISSN 0196-8904, https://doi.org/10.1016/j.enconman.2024.118522.
[5] Roberto Ianniello, Michele Pipicelli, Giuseppe Di Luca, Carlo Beatrice, Gabriele Di Blasio, A study on supercritical water injection as waste heat recovery system in internal combustion engines, Applied Thermal Engineering, Volume 248, Part A, 2024, 123084, ISSN 1359-4311, https://doi.org/10.1016/j.applthermaleng.2024.123084.
[6] Balagurunathan Jayakishan, Sundararajan Rajkumar, G. Nagarajan, Experimental investigation and optimization of dual fuel combustion using diesel/gasoline and Bio-oil extracted from Co-thermal liquefaction of paint/biomass wastes: An approach towards waste to energy, Journal of Cleaner Production, Volume 447, 2024, 141396, ISSN 0959-6526, https://doi.org/10.1016/j.jclepro.2024.141396.
[7] Zengbin Liu, Xudong Zhen, Zhi Tian, Daming Liu, Yang Wang, Study on the effect of injection strategy on the combustion and emission characteristics of direct injection spark ignition bio-butanol engine, Energy, Volume 289, 2024, 129958, ISSN 0360-5442, https://doi.org/10.1016/j.energy.2023.129958.
[8] Shuman Guo, Jiahui Liu, Chuanhao Zhao, Lijun Wang, Zhenzhong Yang, Research on pre-ignition in hydrogen internal combustion engines based on characteristic parameters of hot spot, International Journal of Hydrogen Energy, Volume 65, 2024, Pages 548-554, ISSN 0360-3199, https://doi.org/10.1016/j.ijhydene.2024.03.375.
[9] Yao Lu, Jinhao Que, Mingqiang Liu, Huazhi Zhao, Liyan Feng, Study on backfire characteristics of port fuel injection single-cylinder hydrogen internal combustion engine, Applied Energy, Volume 364, 2024, 123110, ISSN 0306-2619, https://doi.org/10.1016/j.apenergy.2024.123110.

[10] Pier Paolo Brancaleoni, Enrico Corti, Vittorio Ravaglioli, Davide Moro, Giacomo Silvagni, Innovative torque-based control strategy for hydrogen internal combustion engine, International Journal of Hydrogen Energy, Volume 73, 2024, Pages 203-220, ISSN 0360-3199, https://doi.org/10.1016/j.ijhydene.2024.05.481.
[11] Nathália Duarte Souza Alvarenga Santos, Vinícius Rückert Roso, Augusto César Teixeira Malaquias, José Guilherme Coelho Baêta, Internal combustion engines and biofuels: Examining why this robust combination should not be ignored for future sustainable transportation, Renewable and Sustainable Energy Reviews, Volume 148, 2021, 111292, ISSN 1364-0321, https://doi.org/10.1016/j.rser.2021.111292.
[12] Chengda Xing, Xu Ping, Ruilian Guo, Hongguang Zhang, Fubin Yang, Mingzhe Yu, Anren Yang, Yan Wang, Machine learning-based multi-objective optimization and thermodynamic evaluation of organic Rankine cycle (ORC) system for vehicle engine under road condition, Applied Thermal Engineering, Volume 231, 2023, 120904, ISSN 1359-4311, https://doi.org/10.1016/j.applthermaleng.2023.120904.
[13] Nicolae Vlad Burnete, Florin Mariasiu, Christopher Depcik, Istvan Barabas, Dan Moldovanu, Review of thermoelectric generation for internal combustion engine waste heat recovery, Progress in Energy and Combustion Science, Volume 91, 2022, 101009, ISSN 0360-1285, https://doi.org/10.1016/j.pecs.2022.101009.
[14] Leonardo Rodrigues de Araújo, Alexandre Persuhn Morawski, Marcelo Aiolfi Barone, Helder Roberto Oliveira Rocha, João Luiz Marcon Donatelli, José Joaquim Conceição Soares Santos, Response surface methods based in artificial intelligence for superstructure thermoeconomic optimization of waste heat recovery systems in a large internal combustion engine, Energy Conversion and Management, Volume 271, 2022, 116275, ISSN 0196-8904, https://doi.org/10.1016/j.enconman.2022.116275.
[15] Vaclav Novotny, Jan Spale, David J. Szucs, Hung-Yin Tsai, Michal Kolovratnik, Direct integration of an organic Rankine cycle into an internal combustion engine cooling system for comprehensive and simplified waste heat recovery, Energy Reports, Volume 7, Supplement 5, 2021, Pages 644-656, ISSN 2352-4847, https://doi.org/10.1016/j.egyr.2021.07.088.
[16] Xu Ping, Fubin Yang, Hongguang Zhang, Chengda Xing, Baofeng Yao, Yan Wang, An outlier removal and feature dimensionality reduction framework with unsupervised learning and information theory intervention for organic Rankine cycle (ORC), Energy, Volume 254, Part B, 2022, 124268, ISSN 0360-5442, https://doi.org/10.1016/j.energy.2022.124268.
[17] Roberto Pili, Christoph Wieland, Hartmut Spliethoff, Fredrik Haglind, Numerical analysis of feedforward concepts for advanced control of organic Rankine cycle systems on heavy-duty vehicles, Journal of Cleaner Production, Volume 351, 2022, 131470, ISSN 0959-6526, https://doi.org/10.1016/j.jclepro.2022.131470.
[18] Yao Shi, Zhiming Zhang, Xiaoqiang Chen, Lei Xie, Xueqin Liu, Hongye Su, Data-Driven model identification and efficient MPC via quasi-linear parameter varying representation for ORC waste heat recovery system, Energy, Volume 271, 2023, 126959, ISSN 0360-5442, https://doi.org/10.1016/j.energy.2023.126959.
[19] Muhammad Imran, Roberto Pili, Muhammad Usman, Fredrik Haglind, Dynamic modeling and control strategies of organic Rankine cycle systems: Methods and challenges, Applied Energy, Volume 276, 2020, 115537, ISSN 0306-2619, https://doi.org/10.1016/j.apenergy.2020.115537.
[20] Sylvain Quoilin, Richard Aumann, Andreas Grill, Andreas Schuster, Vincent Lemort, Hartmut Spliethoff, Dynamic modeling and optimal control strategy of waste heat recovery Organic Rankine Cycles, Applied Energy, Volume 88, Issue 6, 2011, Pages 2183-2190, ISSN 0306-2619, https://doi.org/10.1016/j.apenergy.2011.01.015.
[21] Matteo Marchionni, Giuseppe Bianchi, Apostolos Karvountzis-Kontakiotis, Apostolos Pesyridis, Savvas A. Tassou, An appraisal of proportional integral control strategies for small scale waste heat to power conversion units based on Organic Rankine Cycles, Energy, Volume 163, 2018, Pages 1062-1076, ISSN 0360-5442, https://doi.org/10.1016/j.energy.2018.08.156.
[22] Imran, M., & Haglind, F. (2019). Dynamic modelling and development of a reliable control strategy of organic Rankine cycle power systems for waste heat recovery on heavy-duty vehicles. In Proceedings of ECOS 2019: 32nd International Conference on Efficiency, Cost, Optimization, Simulation and Environmental Impact of Energy Systems.
[23] Muhammad Usman, Muhammad Imran, Dong Hyun Lee, Byung-Sik Park, Experimental investigation of off-grid organic Rankine cycle control system adapting sliding pressure strategy under proportional integral with feed-forward and compensator, Applied Thermal Engineering, Volume 110, 2017, Pages 1153-1163, ISSN 1359-4311, https://doi.org/10.1016/j.applthermaleng.2016.09.021.
[24] Can Yang, Weiye Wang, Hui Xie, An efficiency model and optimal control of the vehicular diesel exhaust heat recovery system using an organic Rankine cycle, Energy, Volume 171, 2019, Pages 547-555, ISSN 0360-5442, https://doi.org/10.1016/j.energy.2018.12.219.
[25] E. Feru, F. Willems, B. De Jager, M. Steinbuch, Modeling and control of a parallel waste heat recovery system for euro-VI heavy-duty diesel engines, Energies 7 (10) (2014) 6571–6592, https://doi.org/10.3390/en7106571.
[26] J. Peralez, P. Tona, A. Sciarretta, P. Dufour, M. Nadri, Optimal Control of a Vehicular Organic Rankine Cycle via Dynamic Programming with Adaptive Discretization Grid, IFAC Proceedings Volumes, Volume 47, Issue 3, 2014, Pages 5671-5678, ISSN 1474-6670, ISBN 9783902823625, https://doi.org/10.3182/20140824-6-ZA-1003.02185.
[27] J. Peralez, P. Tona, M. Nadri, P. Dufour, A. Sciarretta, Optimal control for an organic rankine cycle on board a diesel-electric railcar, Journal of Process Control, Volume 33, 2015, Pages 1-13, ISSN 0959-1524, https://doi.org/10.1016/j.jprocont.2015.03.009.
[28] J. Zhang, M. Ren and H. Yue, "Constrained entropy-based temperature control of waste heat systems," 2016 12th World Congress on Intelligent Control and Automation *(WCICA)*, Guilin, China, 2016, pp. 1992-1998, doi: 10.1109/WCICA.2016.7578809.
[29] Andres Hernandez, Adriano Desideri, Clara Ionescu, Sylvain Quoilin, Vincent Lemort, Robin De Keyser, Increasing the efficiency of Organic Rankine Cycle Technology by means of Multivariable Predictive Control, IFAC Proceedings Volumes, Volume 47, Issue 3, 2014, Pages 2195-2200, ISSN 1474-6670, ISBN 9783902823625, https://doi.org/10.3182/20140824-6-ZA-1003.01796.
[30] H. Koppauer, W. Kemmetmüller, A. Kugi, Model predictive control of an automotive waste heat recovery system, Control Engineering Practice, Volume 81, 2018, Pages 28-42, ISSN 0967-0661, https://doi.org/10.1016/j.conengprac.2018.09.005.
[31] D. Luong and T. -C. Tsao, "Linear Quadratic Integral control of an Organic Rankine Cycle for waste heat recovery in heavy-duty diesel powertrain," *2014 American Control Conference*, Portland, OR, USA, 2014, pp. 3147-3152, doi: 10.1109/ACC.2014.6858907.keywords: {Mathematical model;Valves;Heat sinks;Heat recovery;Heat engines;Constrained control;Modeling and simulation;Optimal control}.
[32] J. Zhang, T. Zhang, M. Lin, G. Hou and K. Li, "Multiple model predictive control for organic rankine cycle (ORC) based waste heat energy conversion systems," *2016 UKACC 11th International Conference on Control (CONTROL)*, Belfast, UK, 2016, pp. 1-7, doi: 10.1109/CONTROL.2016.7737577.
[33] Yannic Vaupel, Jan C. Schulze, Adel Mhamdi, Alexander Mitsos, Nonlinear model predictive control of organic Rankine cycles for automotive waste heat recovery: Is it worth the effort?, Journal of Process Control, Volume 99, 2021, Pages 19-27, ISSN 0959-1524, https://doi.org/10.1016/j.jprocont.2021.01.003.
[34] J. Peralez, M. Nadri, P. Dufour, P. Tona, A. Sciarretta, Organic rankine cycle for vehicles: control design and experimental results, IEEE Trans. Control Syst. Technol. 25 (3) (2017) 952–965, https://doi.org/10.1109/TCST.2016.2574760.
[35] D. Seitz, O. Gehring, C. Bunz, M. Brunschier, O. Sawodny, Model-based control of exhaust heat recovery in a heavy-duty vehicle, Control Engineering Practice, Volume 70, 2018, Pages 15-28, ISSN 0967-0661, https://doi.org/10.1016/j.conengprac.2017.08.010.
[36] Fabio Fatigati, Arianna Coletta, Marco Di Bartolomeo, Roberto Cipollone, The dynamic behaviour of ORC-based power units fed by exhaust gases of internal combustion engines in mobile applications, Applied Thermal Engineering, Volume 240, 2024, 122215, ISSN 1359-4311, https://doi.org/10.1016/j.applthermaleng.2023.122215.
[37] Fabio Fatigati, Diego Vittorini, Arianna Coletta, Roberto Cipollone, Assessment of the differential impact of scroll and sliding vane rotary expander permeability on the energy performance of a small-scale solar-ORC unit, Energy Conversion and Management, Volume 269, 2022, 116169, ISSN 0196-8904, https://doi.org/10.1016/j.enconman.2022.116169.
[38] Fabio Fatigati, Davide Di Battista, Roberto Cipollone, Permeability effects assessment on recovery performances of small-scale ORC plant, Applied Thermal Engineering, Volume 196, 2021, 117331, ISSN 1359-4311, https://doi.org/10.1016/j.applthermaleng.2021.117331.
[39] M. Marchionni, F. Fatigati, M. Di Bartolomeo, D. Di Battista, M. Petrollese, Experimental and numerical dynamic investigation of an ORC system for waste heat recovery applications in transportation sector, Energies 15 (2022) 9339, https://doi.org/10.3390/en15249339.
[40] Fabio Fatigati, Marco Di Bartolomeo, Davide Di Battista, Roberto Cipollone; Experimental characterization of a hermetic scroll expander operating in an ORC-based power unit bottoming an internal combustion engine. *AIP Conf. Proc.* 17 December 2019; 2191 (1): 020069. https://doi.org/10.1063/1.5138802.
[41] Davide Di Battista, Marco Di Bartolomeo, Carlo Villante, Roberto Cipollone, On the limiting factors of the waste heat recovery via ORC-based power units for on-the-road transportation sector, Energy Conversion and Management, Volume 155, 2018, Pages 68-77, ISSN 0196-8904, https://doi.org/10.1016/j.enconman.2017.10.091.
[42] Qiang Zhang, Yong-Qiang Feng, Kang-Jing Xu, Hui-Jie Liang, Zhi-Nan Liu, Chuang-Yao Zhao, Yong-Zhen Wang, Paul Sapin, Christos N. Markides, Dynamic behaviour and performance evaluation of a biomass-fired organic Rankine cycle combined heat and power (ORC-CHP) system under different control strategies, Applied Thermal Engineering, Volume 248, Part B, 2024, 123236, ISSN 1359-4311, https://doi.org/10.1016/j.applthermaleng.2024.123236.
[43] Jianhua Zhang, Yeli Zhou, Ying Li, Guolian Hou, Fang Fang, Generalized predictive control applied in waste heat recovery power plants, Applied Energy, Volume 102, 2013, Pages 320-326, ISSN 0306-2619, https://doi.org/10.1016/j.apenergy.2012.07.038.
[44] Fabio Dal Magro, Manuel Jimenez-Arreola, Alessandro Romagnoli, Improving energy recovery efficiency by retrofitting a PCM-based technology to an ORC system operating under thermal power fluctuations, Applied Energy, Volume 208, 2017, Pages 972-985, ISSN 0306-2619, https://doi.org/10.1016/j.apenergy.2017.09.054.
[45] R. Pili, S. Eyerer, F. Dawo, C. Wieland, H. Spliethoff, Development of a non-linear state estimator for advanced control of an ORC test rig for geothermal application, Renewable Energy, Volume 161, 2020, Pages 676-690, ISSN 0960-1481, https://doi.org/10.1016/j.renene.2020.07.121.